Diagnostic techniques for photonic materials based on Raman and Brillouin spectroscopies*

M. Mattarelli[1], S.Caponi[1,2], A. Chiappini[1], M. Montagna[1], E. Moser[1], F. Rossi[1],C.Tosello[1], C. Armellini[3], A. Chiasera[3], M. Ferrari[3], Y. Jestin[3], G. Nunzi Conti[4], S. Pelli[4],and G.C. Righini[4,5]**

1 Dipartimento di Fisica, Università di Trento CSMFO group, Trento, Italy

2 INFM CRS-SOFT, c/o Universita' di Roma "La Sapienza", I-00185, Roma, Italy

3 CNR- IFN, Istituto di Fotonica e Nanotecnologie, CSMFO group, Trento, Italy.

4 Photonic Materials and Devices Laboratory, IFAC – CNR, Sesto Fiorentino, Italy.

5 CNR, Department of Materials and Devices, Roma, Italy.

(Received 29 November 2006)

The elastic and vibrational properties of a material, bulk or planar waveguide, are studied by Brillouin and Raman spectroscopy to follow the process of nanocrystals growth in glass-ceramics. The nanoparticles cause the appearance, in the low frequency Raman spectrum, of characteristic peaks, whose position depends on the size of the crystals. At the same time, sharp crystal peaks, due to optical phonons, appear in the Raman spectra, allowing the determination of the nucleated phase, and a frequency shift of the Brillouin peaks is observed.

CLC numbers: TB383 **Document code:** A **Article ID:** 1673-1905(2007)03-0188-04

DOI 10.1007/s11801-007-6197-x

Brillouin and Raman spectroscopies (BS and RS), by exploiting the interaction between light and vibrations, are powerful non-destructive techniques extensively used in pure and applied research to characterize materials. Systems in different state of aggregation, liquids, solids and gases can be studied by RS and BS [1-7]. Also, single molecules have been studied by surface enhanced Raman scattering[8]. The Raman and Brillouin spectra give information on the structure of crystals, glasses and glass-ceramics, show the nature of bonds and give insight on the elastic inhomogeneities caused by pores, nanoparticles and phase separation on various length scales [1,2,6]. In particular RS is a very useful analytic tool, since the vibrating molecular groups (Raman active) have characteristic frequencies.The analysis is also quantitative, the scattered light being proportional to the concentration of such groups.

In optoelectronics, these investigation techniques are widely used both for characterizing crystals, as, for instance, to assess the stoichiometry of $LiNbO_3$ with high resolution [9], or glasses. RS constitutes the main technique to investigate the structure of glasses, lacking the information that X-ray diffraction may give for crystals.

RS with waveguided excitation in a mode of a planar waveguide (WG) has the advantage of obtaining information only on the region of interest, avoiding the contribution of the substrate. Moreover, in a graded index WG, different guided modes propagate at different depths in the guiding film leading to a depth-selective spectroscopic characterization of a WG by RS and BS[10,13].

In a light scattering experiment, the spectral density of the scattered light is given by

$$I(\boldsymbol{q},\omega)\propto\int\langle\delta\varepsilon(\boldsymbol{0},0)\delta\varepsilon(\boldsymbol{r},t)\mathrm{e}^{-i\omega t}\mathrm{e}^{-i\boldsymbol{r}\boldsymbol{q}}\mathrm{d}t\mathrm{d}\boldsymbol{r} \quad (1)$$

where $\boldsymbol{q}$ and $\eta\omega$ are the exchanged wavevector and energy, respectively and $\delta\varepsilon$ is the fluctuation of the dielectric constant. The inelastic light scattering is due to time dependent dielectric constant fluctuations [2,12]. The fluctuations of the dielectric constant may be due to the change of the position of the scatter units and to a change of their polarizabilities, induced by the vibration. This allows to roughly distinguish the different parts of the scattered light spectrum.BS refers to the light scattered by a propagating acoustic wave, is $\boldsymbol{q}$-dependent, and is mainly caused by the displacements of the scatterers. RS refers to optical vibrations, is practically $\boldsymbol{q}$-independent, and is mainly caused by the modulation of the bond polarizability. Low frequency Raman scattering (LFRS) from the symmetric and quadrupolar acoustic vibrations of nanoparticles presents features intermediate between the two,

* The present work has been funded partly with the financial support of MIUR-FIRB RBNE012N3X, MIUR PRIN, PAT FAPVU 2004-2006.

** E-mail:mattarel@science.unitn.it

being ***q***-independent, but with frequency peaks inverse proportional to the size [2,5]. In LFRS is often considered also the boson peak, a feature common to all glasses, related to the presence of electrical and mechanical disorder and with a mixed optical and acoustical nature [14].

Fig.1 shows the different frequency ranges of these inelastic light scattering processes with the Brillouin scattering at frequencies below 2 cm^{-1}, the Raman spectrum at frequency higher than 100 cm^{-1}, and with the boson peak and the peaks due to the scattering of the nanoparticles in between. In the following we discuss some examples of the use of these techniques to study nanostructured materials developed for applications in the field of optical amplification. In particular, Raman and Brillouin spectroscopy give valuable information on the process of growth of nanocrystals by heat treatment of the precursor glass.

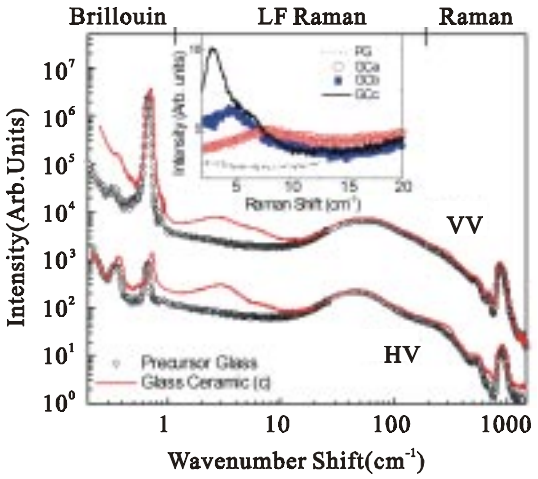

Fig.1 Brillouin and Raman spectra of PG and GCc upon 514.5 nm excitation taken in a 90° scattering geometry. Inset: VV Raman spectra of the PG, GCa, GCb, and GCc samples. The tail of the Brillouin peak was subtracted, and the spectra were normalized in the frequency range of the boson peak.

Rare-earth doped glass–ceramic materials with active ions embedded in the crystalline phase combine the mechanical and optical properties of the glass with a crystal-like environment for the rare-earth ions. An accurate control of the size of the nanocrystals ensures a transparency of glass ceramics comparable to that of the precursor glass at all wavelengths. Furthermore, oxyfluoride glass ceramic, where the nucleated crystalline phase is fluoride, can provide a low-phonon-energy host for the rare earth ions [15,16].

Glass ceramic samples (GCa,GCb, and GCc) were fabricated by heat treatment (see Tab.1) of the precursor glass (PG) with composition 32(SiO_2): 9($AlO_{1.5}$):31.5(CdF_2): 18.5(PbF_2): 5.5(ZnF_2): 3.5(TmF_3) mol% prepared by melt quenching. As observed by XRD and TEM, the nucleated phase is cubic PbF_2 [16].

Fig.1 shows the inelastic light scattering spectra of PG and GCc in a range of about 4 decades from 0.2 to 1500 cm^{-1}. The polarized VV and depolarized HV spectra were obtained by exciting the samples with the 514.5 nm line of an Ar^+-ion laser in a standard 90° geometrical configuration. The signal was analyzed by a double monochromator and detected by a photon-counting system. Two different equipments were employed. The maximum resolution was about 0.5 cm^{-1} for the double monochromator with a 1 m focal length (used for wavenumber larger than 50 cm^{-1}) and 0.03 cm^{-1} for that with a 2 m focal length, working at the eleventh order.

The growth of β -PbF_2 nanoparticles has several effects on the Raman and Brillouin spectra. The peaks corresponding to the silica alumina network (Si-O-Si, Si-O-Al linkages), in the range 800-1200 cm^{-1}, are scarcely affected by the nanoparticle formation. A new broad peak, attributed to the PbF_2 vibration, appears at about 250 cm^{-1} [17].

The most impressive change are in the low frequency region, where the peaks due to symmetric (l=0) and quadrupolar (l=2) surface acoustic vibrations of the nanoparticles appear. Their position is related to the average size of the particles [2]. In the approximation of a free sphere, the frequencies are given by

$$\omega_{0,2}=\frac{S_{0,2}V_{0,2}}{dc} \tag{2}$$

where S_0 and S_2 are constants of the order of unity that depend on the ratio of the longitudinal and transverse sound velocities, $V_0 = V_L$ and $V_2 = V_T$ are the longitudinal and transverse sound velocities, d is the diameter of the nanoparticle, and c is the velocity of light. The interaction of the crystalline nanoparticle with the surrounding glass cause a broadening and a shift of the Raman peaks that must be taken into account for a correct estimation of the mean particle size [2]. The inset of Fig.1 shows that the frequency of the l = 0, 2 peaks decreases with the thermal treatment, indicating an increase of the particles size up to 14 nm, as shown in Tab.1. After ceramming, most of the rare earth ions are embedded in the β -PbF_2 nanocrystals [15].

Brillouin peaks appear in the region below 1 cm^{-1}. In a glass, there are two Brillouin peaks, due to transversal and longitudinal acoustic waves. From their frequency position, the sound velocity (longitudinal and transversal) can be recovered according to the equation [10]:

$$V_{L,T}=\frac{\omega_{L,T}}{q} \text{ with } q=\left(\frac{2n\omega_0}{c}\right)\sin\left(\frac{\varphi}{2}\right) \tag{3}$$

Tab.1 Parameters of the heat treatments, time (t_T) and temperature (T_T), carried out on the oxyfluoride samples, refractive index (n), Brillouin peak frequencies(ω_L, ω_T) and velocities (v_L, v_T) of longitudinal and transversal sound waves, peak frequencies of the l = 0 and 2 acoustic modes, mean size (d_0) of the nanocrystals.

	PG	GCa	GCb	GCc
Heat Treatment (t_T at T_T)		5 h at 400 °C	15' at 440 °C	5 h at 440 °C
n at 514.5 nm (± .001)	1.766	1.774	1.771	1.773
ω_L (± 0.02 cm^{-1})	0.67	0.68	0.69	.705
ω_T (± 0.02 cm^{-1})	0.33	0.33	0.34	0.35
v_L (± 120 m s^{-1})	4130	4170	4240	4330
v_T (± 120 m s^{-1})	2030	2020	2090	2150
ω_2 (cm^{-1})		7.7	4.5	3
ω_0 (cm^{-1})		14	8	5.9
d_0 (nm)		4 ± 1	9 ± 2	14 ± 3

where n is the refractive index of the material, $\eta\omega_0$ is the energy of the exciting photons, and φ is the angle between the exciting and scattered light. Tab.1 shows that the sound velocity increases with ceramming because of the depleting of the heavy lead fluoride from the silica-alumina network, through which mainly travel the sound waves.

Planar WG constitutes a promising format for the integration of multiple functions in a single compact device and sol-gel technique is an established fabrication technique [18]. Silica-titania films with molar composition 85 SiO_2-15 TiO_2 were deposited on SiO_2 substrate by dip coating following the procedure reported in ref.[19]. The thickness (about 2.0 μm) and the refractive index (about 1.53) of the WGs were measured by m-line technique.

The OH presence has detrimental effects on the waveguides, increasing losses due to absorption and reducing the radiative efficiency of the erbium ions in active materials [18]. The water content is usually checked by IR spectroscopy looking at the 3500 cm^{-1} OH stretching vibrations. In waveguides deposited on silica the absorption measurements are not informative because, even for thick films, the substrate would mask the presence of the OH groups in the films. However, since OH 3500 cm^{-1} vibrations are Raman active too, guided RS may be a suitable tool to investigate the water content of the waveguides.

Fig.2 shows the Raman spectra of SiO_2-TiO_2 WGs. After the deposition, the OH band is quite intense but subsequent heat treatments at 900 °C for progressively longer times (up to 45') are effective in reducing it. Moreover, the shape of the OH peak may be investigated to gain insight on the kind of binding of the OH with the glass network (silanol, physical and chemical water) [4].

The heat treatment has effects also on the silica titania network: after heat treatment, sharp peaks appear in the region between 100 and 300 cm^{-1}, and become more intense with increasing duration of treatments. These peaks are due to optical vibrations of crystalline TiO_2. Comparing our spectra with those reported in literature, we found that anatase and brookite phases coexist [20], with an evolution towards the anatase phase; It is possible to follow the progressive growth of the nanocystals by LFRS as previously shown for the bulk materials [19].

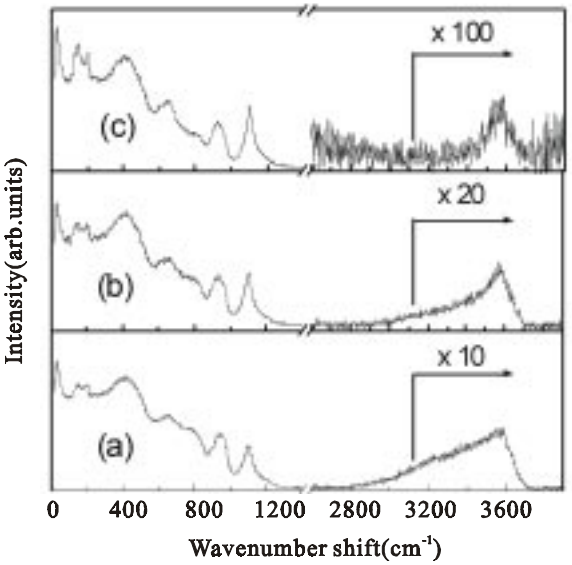

Fig.2 VV polarized Raman spectra of SiO_2-TiO_2 waveguides upon excitation in the TE_0 mode at 457.9 nm for the measurement at frequencies lower than 1300 cm^{-1} (left), and at 514.5 nm for the high frequency region (a) sample as produced, (b) after annealing at 900 ℃ for 15 min, and (c) after annealing at 900 ℃ for 45 min.

The Brillouin scattering in WGs is quite different from the case of a bulk material, because in a waveguide the exciting light beam does not have a single well defined wavevector [10]. A simple model can account for the measured spectra, which are different for different mode excitations, and allows to deduce the sound velocities in films with a step index profile, while more accurate modelling is required in the case of graded index WG [12]. In a ray-optic approach, for

a step-index WG, the exciting light propagates in a zig-zag path and two values q_1 and q_2 of the exchanged wave vector are presented. Therefore, the Brillouin spectrum of the WG shows four peaks in the Stokes and four peaks in the anti-Stokes spectrum. Two peaks are due to longitudinal phonons and the other two to transverse phonons. Fig.3 reports the Brillouin spectra of a thick (3.7 μm) SiO_2-TiO_2 WG upon excitation at 514.5 nm (resolution = 0.04 cm^{-1}). From the peak frequencies, using Eq. (3), it is possible to obtain the values of the sound velocities, V_L= 5.75x10^3 m/s and V_T = 3.46 × 10^3 m/s, which well compare with the available data of silica-titania bulk glasses, obtained by different techniques [21].

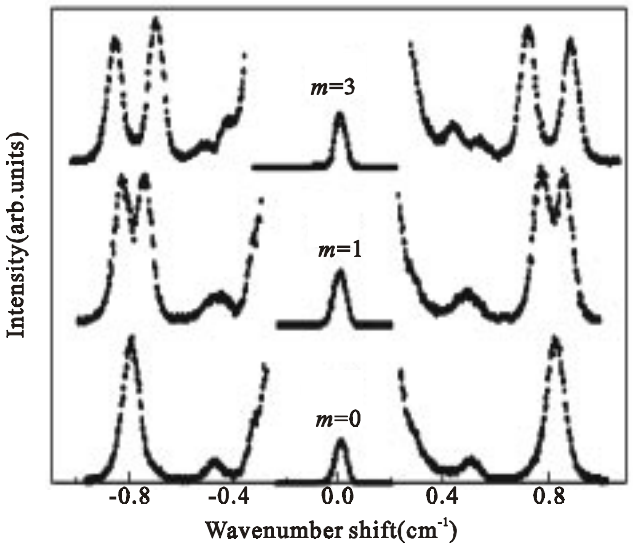

Fig.3 Brillouin spectra of a silica-titania planar waveguide of composition 87SiO_2-13TiO_2 mol % and thickness 3.7 μm, obtained by excitation at 514.5 nm in different TEm modes. The appearance of a single peak in the TE_0 spectrum is due to an interference effect between the light scattered in the zig and zag paths [10].

In conclusion, Raman and Brillouin spectroscopy constitute very effective techniques in investigating glassy and glass-ceramic materials for photonic applications and allow to follow the various stages of the ceramming process.

Acknowledgement

The authors are thankful to Dr. V.K. Tikhomirov for the oxyfluoride samples.

References

[1] S. Caponi, G. Carini, G. D'angelo, A. Fontana, O.Pilla, F. Rossi, E. Terki, and T. Woignier, Phys. Rev. B,**70** (2004), 214204.

[2] M.Montagna and R.Dusi, Phys.Rev.B., **52**(1995), 10080.

[3] D. Fioretto, M. Mattarelli, C. Masciovecchio, G. Monaco, G. Ruocco, and F. Sette, Phys. Rev. B, **65** (2002) ,224205.

[4] M.Montagna "Characterization of Sol-Gel Material by Raman and Brillouin spectroscopies" in S. Sakka ed., Handbook of Sol-Gel science and technology Vol. II, Kluwer Academic Publishers, Boston (2004), 91-117.

[5] M. Mattarelli, M. Montagna, F. Rossi, A. Chiasera and M. Ferrari, Phys.Rev.B, **74** (2006), 10080.

[6] M.Mattarelli, A.Chiappini, M.Montagna , A.Martucci , A. Ribaudo, M.Guglielmi, M.Ferrari,and A.Chiasera, J. Non-Cryst. Sol., **351** (2005), 1759.

[7] K Sentrayan and V. Kushawaha, J. Phys. D: Appl. Phys., **26** (1993), 1554.

[8] K. Kneipp, Y. Wang, H. Kneipp, L. T. Perelman, I. Itzkan, R. R. Dasari, and M. S. Feld, Phys. Rev Lett., **78** (1997), 1667.

[9] M.Mattarelli, S.Sebastiani, J.Spirkova, S.Berneschi, M.Brenci, R.Calzolai, A.Chiasera, M.Ferrari, M.Montagna, G.Nunzi Conti, S.Pelli,and G.C.Righini, Opt. Mat., **28** (2006), 1292.

[10] M. Montagna, M. Ferrari, F. Rossi, F. Tonelli,and C. Tosello,, Phys. Rev. B, **58** (1998), R547.

[11] M. Ferrari, M. Montagna, S. Ronchin, F. Rossi,and G.C. Righini, Appl. Phys. Lett., **75** (1999), 1529.

[12] A. Chiasera, M. Montagna, F. Rossi,and M. Ferrari, J. Appl. Phys., **94** (2003), 4876.

[13] A. Chiasera, M. Montagna, E. Moser, F. Rossi, C. Tosello, M. Ferrari, L. Zampedri, S. Caponi, R.R. Gonçalves, S. Chaussedent, A. Monteil, D. Fioretto, G. Battaglin, F. Gonella, P. Mazzoldi, and G.C. Righini, J. Appl Phys., **94** (2003), 4882.

[14] A.J. Martin and W. Brenig, Phys. Stat. Sol. (b), **64** (1974), 163.

[15] M. Mattarelli, V.K. Tikhomirov, A.B. Seddon, M. Montagna, E. Moser, A. Chiasera, S. Chaussedent, G. Nunzi Conti, S. Pelli, G.C. Righini, L. Zampedri,and M. Ferrari, J. Non-Cryst. Sol., **345&346** (2004), 354.

[16] V.K. Tikhomirov, D. Furniss, A.B. Seddon, I.M. Reaney, M. Beggiora, M. Ferrari, M. Montagna,and R. Rolli, Appl. Phys. Lett., **81** (2002), 1937.

[17] H. E. Lorenzana, J. E. Klepeis, M. J. Lipp, W. J. Evans, H. B. Radousky, and M. van Schilfgaarde, Phys.Rev.B, **56** (1996), 543.

[18] G.C. Righini, S. Pelli, M. Ferrari, C. Armellini, L. Zampedri, C. Tosello, S. Ronchin, R. Rolli, E. Moser, M. Montagna, A. Chiasera, and S.J.L. Ribeiro, Opt. Quant. Elect., **34** (2002), 1151.

[19] M. Montagna, E. Moser, F. Visintainer, L. Zampedri, M. Ferrari, A. Martucci, M. Guglielmi, M. Ivanda, J. Sol-Gel Sci. Tech., **26** (2003), 241.

[20] M.P. Moret, R. Zallen, D.P. Vijay, and S.B. Desu, Thin Solid Films, **366** (2000), 8.

[21] K. Hirao, K. Tanaka, S. Furukawa, and N. Soga, J. Mater. Sci. Lett., **14** (1995), 697.